Rare Metal Materials and Engineering
Volume 53, Issue 1, January 2024
Available online at www.rmme.ac.cn

Science Press

Cite this article as: Wang Liyuan, Jiang Jiali, Wang Dengke, et al. Control of Atomic-Scale Structure and Properties of Metallic Glasses: A Review of Cryogenic Treatment[J]. Rare Metal Materials and Engineering, 2024, 53(01): 78-84. DOI: 10.12442/j.issn.1002-185X.E20230738.

REVIEW

Control of Atomic-Scale Structure and Properties of Metallic Glasses: A Review of Cryogenic Treatment

Wang Liyuan[1], Jiang Jiali[2], Wang Dengke[1], Zhang Yi[1], Wang Qing[1], Lu Jian[2]

[1] Institute of Materials, Shanghai University, Shanghai 200444, China; [2] Department of Mechanical Engineering, City University of Hong Kong, Hong Kong 999077, China

Abstract: The control of atomic-scale structure of metallic glasses (MGs) to improve their physical, chemical, and mechanical properties is an essential issue. Over past decades, large efforts have been devoted into the development of effective MG control approaches, such as the cryogenic treatment (CT) technique. This research reviewed the effects of cryogenic treatment on the properties and their dependence on the initial structural energy state of MGs. Then, it focused on the atomic-scale structure evolution in MGs during CT, which is of fundamental importance to understand CT effects.

Key words: atomic-scale structure; properties; cryogenic treatment; metallic glass

Because of the lack of long-range periodic structure, metallic glasses (MGs) usually exhibit excellent mechanical, physical, and chemical properties[1–3]. However, their structural application is severely impeded by the limited tensile plasticity at room temperature. Nevertheless, the homogenous-like plastic deformation may occur in compression via multiple shear banding for the glassy alloys[4–5]. Therefore, the control of atomic structure of MGs attracts much attention, which is beneficial to simultaneously initiate and/or multiply shear bands to distribute plasticity in the amorphous structure, even in tension[6–7]. Various effective methods have been developed, such as cold rolling[8–12], high pressure torsion[13–15], elastostatic loading[16–21], thermal recovery treatment[22], high pressure thermal treatment[23–24], and microalloying[23–26].

In recent years, cryogenic treatment (CT) technique attracts much attention for MGs, because CT can effectively control the structural energy state of MGs and MG matrix composites[21,27–40]. As a result, CT technique is an effective method to control the mechanical[21,27–31,33–36,38,40], physical[41–43], and chemical[44] properties of MGs. Experiment and simulation results suggest that the effects of CT are closely related to structural heterogeneity[45–51], which is an intrinsic characteristic for the glassy materials and the key factor to improve the mechanical performance with appropriate tensile plasticity[29]. According to Ref.[47,52], the structural change caused by the nonuniform atomic structure, such as the soft spots typically attached to the nearest neighbor atoms, may occur in MGs, where individual irreversible local atomic rearrangements (shears) can be triggered even in the nominally elastic strain regime. Specifically, for MGs subjected to cryothermal cyclic treatment, significant nano-fluctuation of coefficient thermal expansion, which is closely related to the intrinsic nonuniformity of glassy structure, may induce the atomic-level shear, and the resultant local nonaffine strain promotes the local structural change upon the temperature change[29].

CT is a nondestructive technique, and it can be used to modify the whole structure of any sample (thin film, ribbon, or bulk) without changing their shape[29]. Moreover, unlike the conventional severe plastic deformation, such as surface mechanical attrition treatment[6], shot-peening[53], or elastostatic loading[18–19], MGs treated by CT method only undergo strains far below the limit value, avoiding macroscopic plastic flow. Thus, no significant residual stress or structural anisotropy can be introduced into the samples[29].

According to Ref.[29,54–55], CT technique can be divided into two types: cyclic CT and static CT[29,54–55]. As for cyclic CT, thermal cycling of MGs is performed between the room temperature (far away from glass transition temperature, T_g) or

Received date: November 19, 2023
Foundation item: National Natural Science Foundation of China (52171161); Space Utilization System of China Manned Space Engineering 522 (KJZ-YY-NCL08)
Corresponding author: Wang Qing, Ph. D., Institute of Materials, Shanghai University, Shanghai 200444, P. R. China, E-mail: qingwang@shu.edu.cn

a relatively higher temperature and the liquid nitrogen temperature. As for static CT, MGs are usually held at liquid nitrogen temperature for a long duration to sufficiently change the structural energy state[39,54].

In this review, the research progress on experiment results of the effect of CT on the properties of MGs was reviewed, as well as their dependence on the initial structural state. The CT-induced atomic structural evolution and the responsible mechanism of CT effects were also discussed.

1 Effect of CT on Mechanical Properties of MGs

As demonstrated in Ref. [21, 29, 31–34, 40, 54], CT can lead to a remarkable variation in mechanical properties, such as room-temperature plastic strain for various MG systems (Zr[21,29,31,33–34], Cu[29,32,56], Ti[54], and Pd[40] based glassy alloys). Although most MGs exhibit the increasing plastic strain with prolonging the time or increasing the thermal cycles during CT, others even do not show the degradation in plasticity[33].

Ketov et al[29] conducted thermal cycling on $Cu_{46}Zr_{46}Al_7Gd_1$ bulk MG (BMG), $Zr_{62}Cu_{24}Fe_5Al_9$ BMG, and $La_{55}Ni_{20}Al_{25}$ melt-spun MG ribbon between near room temperature and liquid nitrogen temperature (77 K). Regardless of the chemical composition, the mechanical properties are enhanced for all MG samples after thermal cycling treatment. As shown in Fig. 1a and 1b, compared with those of the as-cast $La_{55}Ni_{20}Al_{25}$ alloy sample, the median value of initial yield pressure P_y and hardness H decrease after cycling treatments by approximately 20% and 5%, respectively. Meanwhile, the plastic strain of BMG samples increases after the treatment. As shown in Fig. 1c, the engineering stress increases from 1.4% to 5.1% for the as-cast $Cu_{46}Zr_{46}Al_7Gd_1$ BMG after 10 cycles of treatment between room temperature and 77 K. Similar effects of thermal cycling between room temperature and 77 K have also been found for other MG systems[29].

Guo et al[31] investigated the effect of cycling treatment from cryogenic temperature to room temperature on the mechanical properties of Zr-based MG. It is found that the plastic compressive strain increases, whereas the hardness decreases after CT. Compared with the as-cast sample, a rejuvenation behavior can be observed for the as-treated MG with increased relaxation enthalpy and reduced density. The monolithic amorphous structure remains even after 40 CT cycles.

However, Guo et al[32] also reported that the MG samples with slight rejuvenation behavior and heterogeneous structure unusually show the high plastic strain of 7.3%, and those with obvious rejuvenation behavior have plastic strain of 2.6%–2.8%. Such enhancement in plasticity results from the stress-induced crystallization of the less stable glassy phase, where more nano-clusters are formed with slow cooling rate[32]. Furthermore, Wang et al[54] conducted the thermal cycling treatment on $Ti_{41}Zr_{25}Be_{29}Al_5$ BMG from −196 °C to 150 °C. It is found that the plastic strain of CT-treated Ti-based BMG barely changes, no embrittlement occurs, and the structural relaxation enthalpy is reduced with increasing the cycling number. Therefore, the reduction in structural relaxation enthalpy is related to the excess free volume of glassy alloys, and it does not necessarily cause the embrittlement of BMGs. Recently, Guo et al[40] observed an inconspicuous rejuvenation behavior of Pd-based BMG during deep cryogenic cycling treatment (DCT). Unlike the Zr-based BMG[31], the Pd-based glassy alloy exhibits slight change in the relaxation enthalpy, hardness, and mechanical properties after thermal cycling.

Ketov et al[33] conducted thermal cycling treatment on $Zr_{60}Cu_{20}Fe_{10}Al_{10}$, $Zr_{60}Cu_{20}Ni_{10}Al_{10}$, and $Zr_{60}Cu_{20}Co_{10}Al_{10}$ MGs, and found that the compressive plastic strain of the samples cannot be increased infinitely with increasing the number of cycles. After 30 thermal cycles, the plasticity of $Zr_{60}Cu_{20}Ni_{10}Al_{10}$ BMG barely changes, whereas the plasticity begins to decrease for the $Zr_{60}Cu_{20}Co_{10}Al_{10}$ BMG, as shown in Fig.2.

Subsequently, Ketkaew et al[38] examined the effects of thermal cycling for various BMGs, such as $Zr_{44}Ti_{11}Cu_{10}Ni_{10}Be_{25}$, $Pd_{43}Cu_{27}Ni_{10}P_{20}$, $Pt_{57.5}Cu_{14.7}Ni_{5.3}P_{22.5}$, and $La_{55}Al_{25}Ni_{20}$ alloys, at different temperatures and found a nonmonotonic change in fracture toughness with increasing the cycling number. For example, the fracture toughness K_Q of the Pd-based BMG at fracture temperature T_f=633 K, which is determined as 38.0±1.0 MPa·m$^{1/2}$ for the as-prepared BMG, increases by 45% and reaches the maximum value of 56±5 MPa·m$^{1/2}$ after approximately 200 thermal cycles[38]. However,

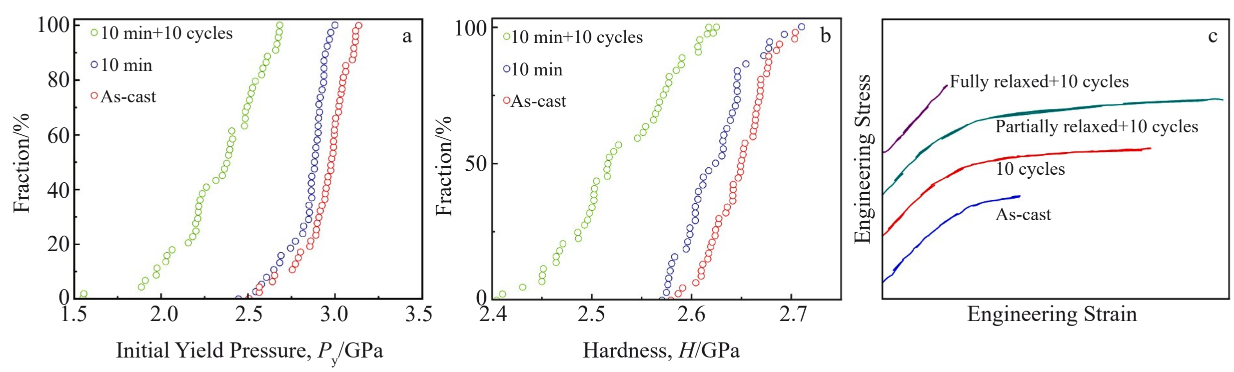

Fig.1 Statistic analysis results of initial yield pressure P_y (a) and hardness H (b) of $La_{55}Ni_{20}Al_{25}$ MG ribbon; engineering stress-engineering strain curves of $Cu_{46}Zr_{46}Al_7Gd_1$ BMG after different treatments under uniaxial compression (c)[29]

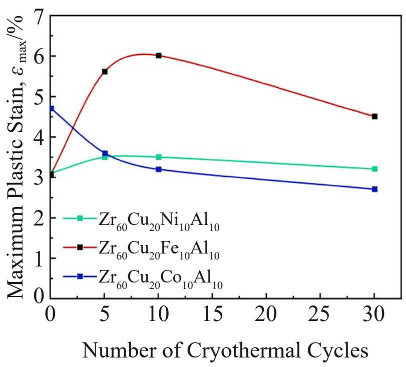

Fig.2 Relationship between maximum plastic strain ε_{max} and the number of cryothermal cycles for different MGs[33]

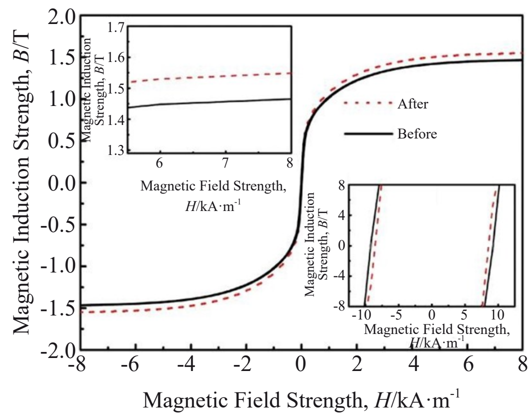

Fig.3 Magnetization property curves of melt-spun $Fe_{80}Si_{8.75}B_{10}Cu_{1.25}$ MG ribbons before and after thermal cycling[42]

with further increasing the number of thermal cycles to 300, K_Q is decreased to 39±5 MPa·m$^{1/2}$, which is comparable to the original value. Similar reversal from rejuvenated state to relaxed state can be observed for other BMGs[38]. It is apparent that the variation in fracture toughness K_Q of the treated BMG sample is closely related to the thermal cycling-induced structural changes.

2 Effect of CT on Physical Properties of MGs

It is known that Fe- or Co-based MGs have superior soft-magnetic properties, such as high magnetization saturation (B_s) and low coercive force (H_c). Moreover, their magnetic properties can be further improved via cryogenic thermal cycling treatment[42–43]. Meng et al[42] measured the soft-magnetic properties (B_s and H_c) for $Fe_{80}Si_{8.75}B_{10}Cu_{1.25}$ MG ribbon before and after insertion into liquid nitrogen for 12 h and then held at room temperature in air for 12 h. As shown in Fig. 3, thermal cycling treatment increases the magnetization saturation B_s of as-spun Fe-based glassy ribbons by about 6.2% from 1.46±0.01 T to 1.55±0.01 T, whereas the coercive force H_c decreases by about 7.3% from 9.2±0.1 A/m to 8.5±0.1 A/m[42]. Zhao et al[43] investigated the effect of cyclic rapid cooling treatment on the magnetic properties and giant magnetoimpedance (GMI) properties for Co-based MG ribbons through the combination of Asylum Research MFP-3D magnetic force microscope, atomic force microscope, and four-terminal contact using impedance analyzer (Agilent 4294 A). It is found that the CT-treated ribbon sample exhibits significant increase in GMI ratio from 80% to 130% at 1 MHz and to 321% at 5 MHz, and the saturation magnetization is improved by cycle treatment[43].

3 Effect of CT on Chemical Properties of MGs

In addition to mechanical and physical properties, chemical properties of MGs also vary with cryogenic thermal cycling. Gu et al[44] reported the dependence of corrosion resistance of $Ti_{50}Zr_{20}Be_{20}Ni_{10}$ BMG in 3.5wt% NaCl solution on structural relaxation and cryogenic thermal cycling. It is found that CT remarkably degrades the corrosion resistance of the Ti-based BMG, and the as-annealed Ti-based BMG displays enhanced corrosion resistance, which can be associated with the high pitting potentials and low corrosion current densities. Furthermore, the analytical results of electrochemical impedance spectra indicate that less stable passive films form on the sample surfaces, whereas the cryogenic thermal cycling induces more free volume of the as-treated BMG. Therefore, it is proposed that the cryogenic treatment can generate more excessive free volume and thus deteriorate the stability of surface passive film of the Ti-based BMG[44].

4 Dependence of CT Effect on Initial Structural State

To clarify the key factors for the control of CT effect, different researches have been conducted on the influence of initial structural state of MGs on the CT effect[21,35–37]. The initial structural state of MG can be associated with the chemical composition[33] and secondary phase[36–37], and it can be modified via thermomechanical treatment, such as physical aging[35] and pre-static elastic loading[21].

To further investigate the mechanism responsible for the rejuvenation effects of MGs, Kang et al[35] studied the compressive plastic behavior with atomic-scale structure evolution in $Zr_{46}Cu_{38}Al_8Ag_8$ MG during thermal cycling treatment at 0.9T_g for 12, 20, and 240 h. It is interesting that the sample with intermediate structure after thermal cycling for 20 h exhibits relatively high degree of rejuvenation effect, compared with that after thermal cycling for 12 and 240 h[35]. As a result, the plasticity increases from 0% to 0.21%±0.10% after thermal cycling for 20 h, and the sample after thermal cycling for 240 h shows discernible plasticity[35]. Moreover, the sample after thermal cycling for 20 h shows less relaxed state than that after thermal cycling for 2 h, as indicated by the relatively higher plastic strain ε_p and yield stress[35].

Ri et al[36] examined the internal residual strain and structural change in the partially-crystallized Fe-based MGs after cryogenic thermal cycling and found that the crystals are under hydrostatic tension and the glasses are under pressure. The presence of Fe_3Si phase induces the residual volumetric strain of 0.08% – 0.21%, which is 12% – 32% of the total volumetric contraction due to the rapid cooling and residual stress. In addition, as a result of cryogenic thermal cycling, the energy of the MG samples increases by 5−50 mJ/g, which is smaller than the energy change measured by DSC[36]. Consequently, Ri et al[36] provided compelling evidence that the structural heterogeneity plays a crucial role in the CT-induced irreversible structural changes and rejuvenation behavior.

Abrosimova et al[37] revealed the influence of the secondary nanocrystal phase in Al-based alloy on CT effect. It is found that cryogenic cycling may lead to the amorphization of nanocrystalline regions and the amorphous phase rejuvenation in the partially crystallized samples. The rejuvenation degree of amorphous phase and the amorphization in crystalline phases are increased with prolonging the CT duration[37]. It is also worth noting that the amorphization of nanocrystal under cryogenic treatment involves the mass transfer, and the chemical composition of nanocrystals differs from that of amorphous phases[37].

Samavatian et al[21] rejuvenated the $Zr_{55}Cu_{30}Al_{10}Ni_5$ BMG by the combination of elastostatic loading and CT interaction. The maximum stored energy of the samples after cryothermal treatment and elastostatic loading is 0.52 and 0.73 kJ/mol, respectively. The samples after the combination treatment of these two thermal mechanical processes have the stored energy of 0.92 kJ/mol[21]. In other words, the elastostatic loading is beneficial to the extra rejuvenation for the Zr-based BMG under CT process.

5 Effect of CT on Glassy Atomic Structure and Energy State

To rationalize the CT effects of MGs, the microstructural evolution during immersion[57] or the thermal cyclic number during CT has been widely researched[33]. Based on different CT processing conditions and/or chemical composition[58–60], MGs undergo various atomic-scale structure change related to the structural rejuvenation[21,33,61], relaxation[41], crystallization[62], or devitrification[63]. These findings are essentially important to understand the CT effects in glassy alloys.

Ketov et al[33] studied the atomic structure evolution in $Zr_{60}Ni_{20}Fe_{10}Al_{10}$ BMG during CT process. As shown in Fig.4, both radial distribution functions calculated from FFT and SAED patterns display the variation of $G(r)$ intensity, whereas the peak positions remain unchanged. Nevertheless, due to the thermal cycling, all radial distribution function peaks shift towards the higher radius value, indicating that the average atomic bonding distance and the general volume of Fe-containing glassy alloy are increased.

Samavatian et al[21] rejuvenated the $Zr_{55}Cu_{30}Al_{10}Ni_5$ BMG by the combination process of elastostatic loading and cryothermal treatment. According to the pair distribution function analysis, the rejuvenation evolution during CT process is accompanied by the annihilation of Cu-rich clusters, the increase in Al-rich clusters, and the intensification of spatial connectivity. However, extensive disordering at both the short range and medium range scales occurs during the tensile elastostatic loading, as shown in Fig.5[21].

Kang et al[35] employed Synchrotron XRD analysis to investigate the atomic-scale structure evolution in $Zr_{46}Cu_{38}Al_8Ag_8$ MG during thermal cycling treatment at $0.9T_g$ for different durations. It is found that thermal cycling treatments for 2 and 20 h decrease the first peak intensities of both structural factor $S(q)$ and radial distribution function $G(r)$, whereas those of MGs after thermal cycling treatment for 240 h barely change, as shown in Fig.6. This result suggests that the CT-induced rejuvenation is related to the structural disordering, and therefore with prolonging the thermal annealing duration, the rejuvenation effect of the Zr-based MG is decreased.

Through the neutron diffraction method, Dokukin et al[41] observed the changes in total structure factor and the total pair correlation function for $Fe_{78}Cu_1Nb_4B_{3.5}Si_{13.5}$ MG caused by CT process. As shown in Fig.7a, the changes in the atomic density is associated with the interatomic distances of short-range order of approximately 0.4 nm. It is evident that CT can cause atom redistribution and reduce the distance between atoms. In the atom distance range of 0.2 nm, the sample after CT process has higher atomic density, implying the occurrence of structural relaxation associated with the atomic redistribution within the first coordination.

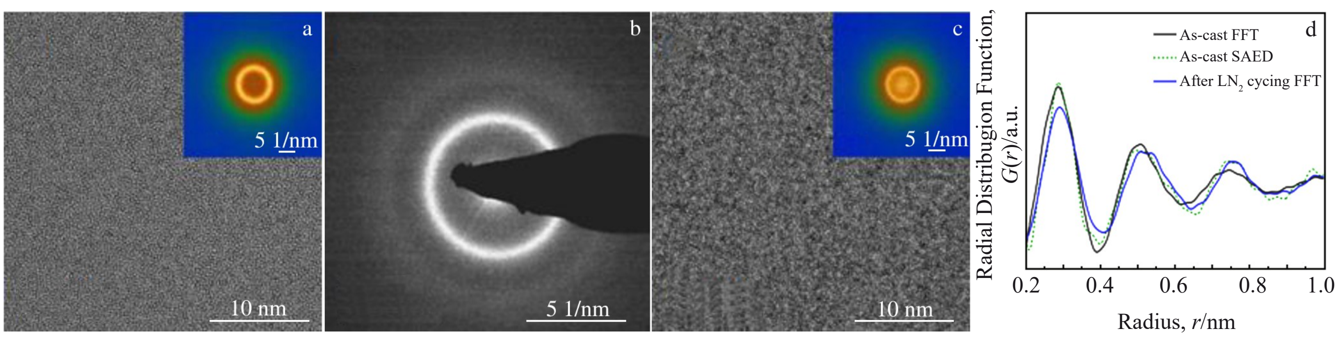

Fig.4 HRTEM images of as-cast $Zr_{60}Ni_{20}Fe_{10}Al_{10}$ BMG before (a) and after (c) 10 cryothermal cycles with corresponding FFT patterns; SAED pattern corresponding to Fig.4a (b); radial distribution functions derived from SAED and FFT patterns (d) [33]

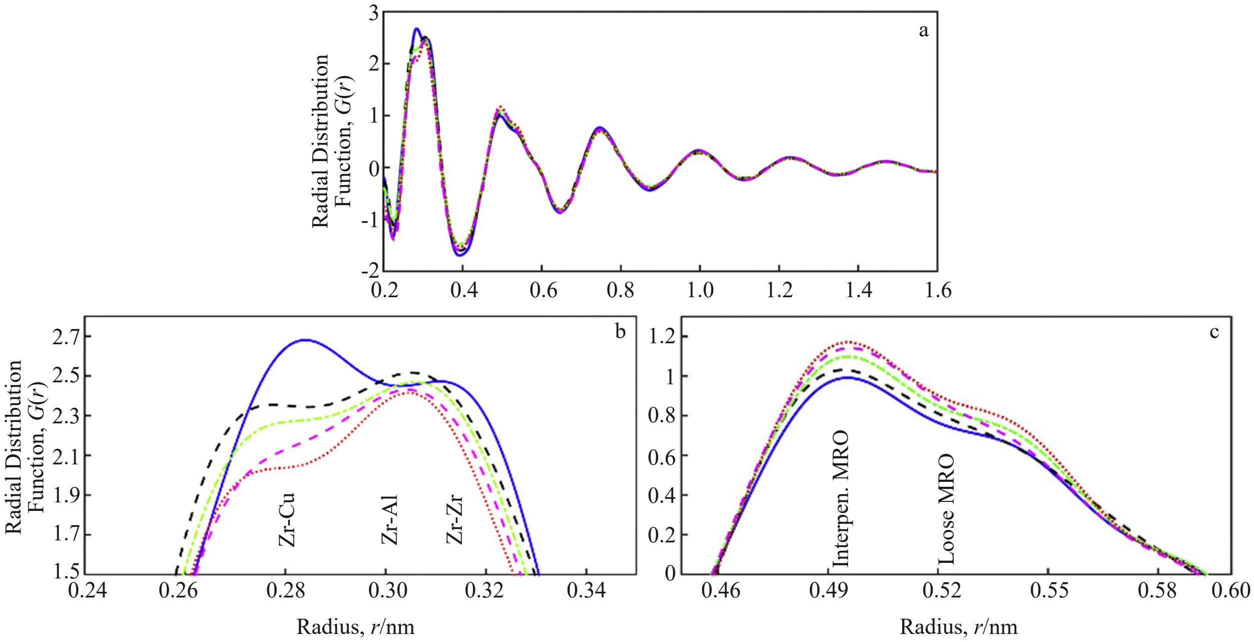

Fig.5 Comparison of radial distribution functions derived from synchrotron XRD results of $Zr_{55}Cu_{30}Al_{10}Ni_5$ BMG after cryothermal treatment for different durations (a); enlarged images of SRO peak (b) and the first MRO peak (c) in Fig.5a[21]

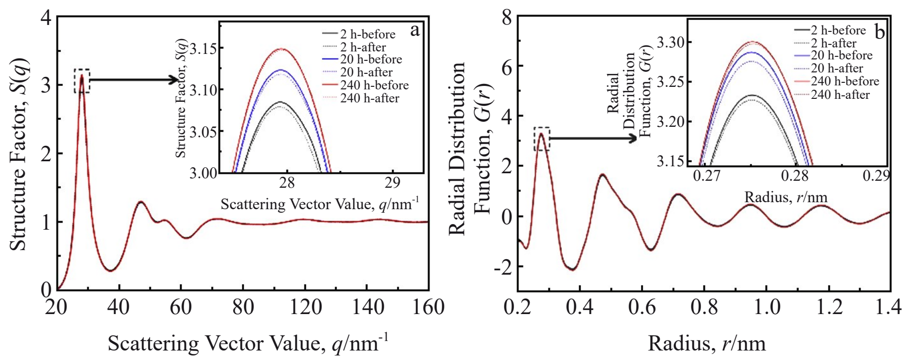

Fig.6 Structure factor (a) and reduced radial distribution function (b) of $Zr_{46}Cu_{38}Al_8Ag_8$ MG before and after thermal cycling for different durations[35]

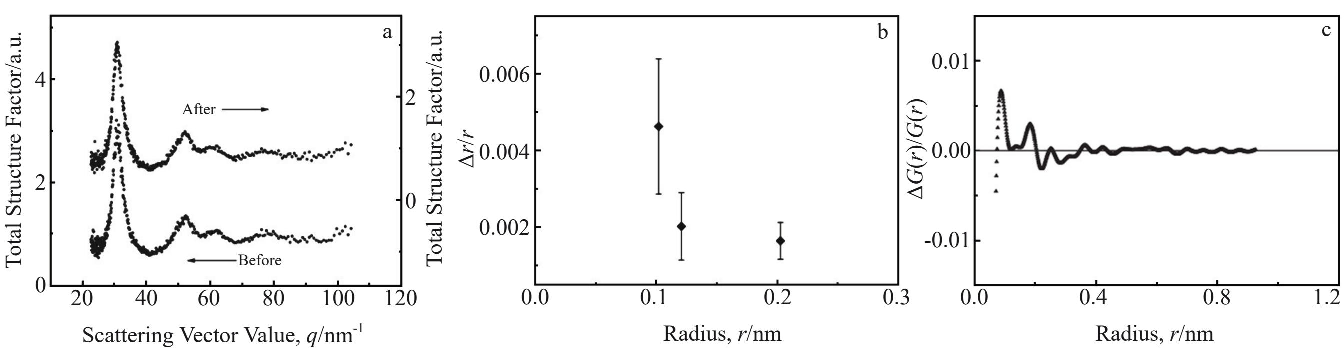

Fig.7 Total structure factor of $Fe_{78}Cu_1Nb_4B_{3.5}Si_{13.5}$ MG before and after CT for 3 h (a); relative change of interatomic spacing after CT for 3 h (b); relative difference of total radial correlation functions of samples before and after CT for 3 h (c)[41]

6 Summary

It is proved that the thermal cycling between room temperature and liquid nitrogen temperature can rejuvenate the metallic glasses (MGs) and therefore remarkably enhance the plasticity. Such cryogenic treatment (CT) effect results from the intrinsic non-uniformity of the glass structure. During the cyclic CT with a large difference in the temperature range, the nonuniform distribution of density, elastic constant, and coefficient of thermal expansion may create high local atomic stress to induce irreversible atomic rearrangements at the plastic flow defects or units. In theory, the resultant high degree of structural disorder and heterogeneity is favorable for the enhancement of plasticity for MGs.

To further investigate the CT-induced variations in atomic structure, energy state, and properties, the dependence of CT effect on the chemical composition, secondary phase, physical aging, and pre-static elastic loading is discussed. In addition to the treatment conditions (cyclic number, temperature range), CT effect of MGs may depend on their chemical composition and initial structural energy state. In other words, CT effects of MGs is closely related to the initial excess free volume, internal stress, or structural heterogeneity.

During CT process, MG usually exhibits complex rejuvenation or structural relaxation behavior, as indicated by the noticeable fluctuation of the curves of relaxation enthalpy or the nearest neighboring atomic structure parameters (coordination number of atoms) versus treatment time or cyclic number. Such CT-induced nonmonotonic changes cannot be well explained by current theory or model. Additionally, the role of excess free volume, short-range atomic structure, nanocrystal or secondary phases in CT effects should also be considered. Consequently, new structural energy state should be focused to investigate the characteristics and properties of glassy alloys during CT process.

More efforts should be devoted to the following critical issues: (1) the intrinsic relationship between the physical or mechanical properties and the atomic mobility or dynamic structural heterogeneity; (2) the influence of chemical component and initial structural energy state on the kinetic behavior of structural rejuvenation or relaxation; (3) the role of excess free volume, short-medium range atomic ordering, and internal stress (elastic) heterogeneity in MGs during CT process.

References

1 Johson W L. *MRS Bulletin*[J], 1999, 24(10): 42

2 Wang W H, Dong C, Shek C H. *Materials Science and Engineering R: Reports*[J], 2004, 44(2–3): 45

3 Schroers J. *Advanced Materials*[J], 2010, 22(14): 1566

4 Schuh C, Hufnagel T, Ramamurty U. *Acta Materialia*[J], 2007, 55(12): 4067

5 Greer A L, Cheng Y Q, Ma E. *Materials Science and Engineering R: Reports*[J], 2013, 74(4): 71

6 Wang Q, Yang Y, Jiang H *et al*. *Scientific Reports*[J], 2014, 4(1): 4757

7 Wang S, Ye Y F, Shi S O *et al*. *Journal of Applied Physics*[J], 2016, 119(24): 245113

8 Cao Q P, Liu J W, Yang K J *et al*. *Acta Materialia*[J], 2010, 58(4): 1276

9 Song K K, Pauly S, Zhang Y *et al*. *Intermetallics*[J], 2011, 19(10): 1394

10 Park J M, Lim K R, Park E S *et al*. *Journal of Alloys and Compounds*[J], 2014, 615: S113

11 Scudino S, Surreddi K B. *Journal of Alloys and Compounds*[J], 2017, 708: 722

12 Li B S, Scudino S, Gludovatz B *et al*. *Materials Science and Engineering A*[J], 2020, 786: 139396

13 Révész Á, Schafler E, Kovács Z. *Applied Physics Letters*[J], 2008, 92(1): 11910

14 Meng F Q, Tsuchiya K, Seiichiro Il *et al*. *Applied Physics Letters*[J], 2012, 101(12): 121914

15 Wang Y B, Qu D D, Wang X H *et al*. *Acta Materialia*[J], 2012, 60(1): 253

16 Lee S C, Lee C M, Lee J C *et al*. *Applied Physics Letters*[J], 2008, 92(15): 151906

17 Park K W, Wakeda M, Shibutani Y *et al*. *Metals and Materials International*[J], 2008, 14(2): 159

18 Park K W, Lee C M, Wakeda M *et al*. *Acta Materialia*[J], 2008, 56(19): 5440

19 Park K W, Lee C M, Kim H J *et al*. *Materials Science and Engineering A*[J], 2009, 499(1–2): 529

20 Greer A L, Sun Y H. *Philosophical Magazine*[J], 2016, 96(16): 1643

21 Samavatian M, Gholamipour R, Amadeh A A *et al*. *Journal of Non-crystalline Solids*[J], 2019, 506: 39

22 Wakeda M, Saida J, Li J. *Scientific Reports*[J], 2015, 5(1): 10545

23 Yamada R, Shibazaki Y, Abe Y *et al*. *NPG Asia Materials*[J], 2019, 11(1): 72

24 Shibazaki Y, Yamada R, Saida J *et al*. *Communications Materials*[J], 2020, 1(1): 53

25 Chen L Y, Fu Z D, Zhang G Q *et al*. *Physical Review Letters*[J], 2008, 100(7): 75501

26 Wang X, Cao Q P, Chen Y M *et al*. *Acta Materialia*[J], 2011, 59(3): 1037

27 Lei T J, Da Costa L R, Liu M *et al*. *Acta Materialia* [J], 2019, 164: 165

28 Priezjev N V. *Journal of Non-crystalline Solids*[J], 2019, 503–404: 131

29 Ketov S V, Sun Y H, Nachum S *et al*. *Nature*[J], 2015, 524(7564): 200

30 Bu F, Wang J, Li L Y *et al*. *Metals*[J], 2016, 6(11): 274

31 Guo W, Yamada R, Saida J. *Intermetallics*[J], 2018, 93: 141

32 Guo W, Yamada R, Saida J *et al*. *Journal of Non-crystalline Solids*[J], 2018, 498: 8

33 Ketov S V, Trifonov A S, Ivanov Y P *et al*. *NPG Asia Materials*[J], 2018, 10(4): 137

34 Guo W, Shao Y M, Saida J *et al*. *Journal of Alloys and Compounds*[J], 2019, 795: 314

35 Kang S J, Cao Q P, Liu J *et al*. *Journal of Alloys and Compounds*[J], 2019, 795: 493

36 Ri M C, Sun Y H, Xue Z Y *et al*. *Journal of Alloys and*

Compounds[J], 2019, 781: 357
37 Abrosimova G, Volkov N, Pershina E *et al*. *Journal of Non-crystalline Solids*[J], 2020, 528: 119751
38 Ketkaew J, Yamada R, Wang H *et al*. *Acta Materialia*[J], 2020, 184: 100
39 Zhang W, Xiang Q C, Ma C Y *et al*. *Journal of Alloys and Compounds*[J], 2020, 825: 153997
40 Guo W, Saida J, Zhao M *et al*. *Materials Science and Engineering A*[J], 2019, 759: 59
41 Dokukin M E, Perov N S, Dokukin E B *et al*. *Physica B: Condensed Matter*[J], 2005, 368(1–4): 267
42 Meng Y, Wang Y G, Zhu L *et al*. *Journal of Non-crystalline Solids*[J], 2017, 471: 406
43 Zhao C, Pan L, Ma X *et al*. *Journal of Magnetism and Magnetic Materials*[J], 2017, 444: 198
44 Gu J, Shao Y, Shi L *et al*. *Intermetallics*[J], 2019, 110: 106467
45 Hufnagel T C, Ott R T, Almer J. *Physical Review B*[J], 2006, 73(6): 64204
46 Ding J, Cheng Y Q, Ma E. *Applied Physics Letters*[J], 2012, 101(12): 121917
47 Ding J, Patinet S, Falk M L *et al*. *Proceedings of the Natlional Academy of Sciences*[J], 2014, 111(39): 14052
48 Wang B, Gao X Q, Qiao J C. *Rare Metal Materials and Engineering*[J], 2024, 53(1): 70
49 Ye J C, Lu J, Liu C T *et al*. *Nature Materials*[J], 2010, 9(8): 619
50 Liu Y H, Wang D, Nakajima K *et al*. *Physical Revview Letters*[J], 2011, 106(12): 125504
51 Wagner H, Bedorf D, Kuchemann S *et al*. *Nature Materials*[J], 2011, 10(6): 439
52 Egami T, Iwashita T, Dmowski W. *Metals*[J], 2013, 3(1): 77
53 Zhang Y, Wang W H, Greer A L. *Nature Materials*[J], 2006, 5(11): 857
54 Wang X, Shao Y, Gong P *et al*. *Journal of Alloys and Compounds*[J], 2013, 575: 449
55 Hufnagel T C. *Nature Materials*[J], 2015, 14(9): 867
56 Guo W, Yamada D, Saida E. *Materials Science and Engineering A*[J], 2017, 699: 81
57 Zhang N Z, Bian X L, Ren C *et al*. *Journal of Alloys and Compounds*[J], 2022, 894: 162407
58 Gong P, Yin G, Jamili-Shirvan Z *et al*. *Materials Science and Engineering A*[J], 2020, 797: 140078
59 Guo W, Shao Y M, Zhao M *et al*. *Journal of Alloys and Compounds*[J], 2020, 819: 152997
60 Di S, Wang Q, Yang Y *et al*. *Journal of Materials Science & Technology*[J], 2022, 97: 20
61 Liang S Y, Zhang L T, Wang B *et al*. *Intermetallics*[J], 2024, 164: 108115
62 Xue P, Huang Y, Pauly S *et al*. *Journal of Alloys and Compounds*[J], 2021, 871: 159570
63 Guo W, Saida J, Zhao M *et al*. *Journal of Materials Science*[J], 2019, 54(11): 8778

金属玻璃原子尺度结构和性能的调控:关于深冷处理的综述

王丽媛[1]，姜佳丽[2]，王登科[1]，张　祎[1]，王　庆[1]，吕　坚[2]
(1. 上海大学 材料研究所，上海 200444)
(2. 香港城市大学 机械工程系，香港 999077)

摘　要：通过调控金属玻璃的原子尺度结构进而提高它们的力学、物理、化学性能极为重要。在过去几十年里，金属玻璃领域研究者投入了大量精力以开发有效调控方法，如深冷处理。本文综述了深冷处理对金属玻璃性能的影响及其对初始结构能量状态的依赖关系，聚焦了金属玻璃中原子结构随深冷处理的演化，这些内容对于深入理解金属玻璃深冷处理效应具有重要作用。
关键词：原子尺度结构；性能；深冷处理；金属玻璃

作者简介：王丽媛，女，1999年生，硕士生，上海大学材料研究所，E-mail：wangly2323@163.com